Human Molecular Genetics, 2006, Vol. 15, No. 5 ***751–765***
doi:10.1093/hmg/ddi490
Advance Access published on January 24, 2006

The *DFNB31* gene product whirlin connects to the Usher protein network in the cochlea and retina by direct association with USH2A and VLGR1

Erwin van Wijk[1], Bert van der Zwaag[4], Theo Peters[1], Ulrike Zimmermann[5], Heleen te Brinke[1], Ferry F.J. Kersten[1], Tina Märker[6], Elena Aller[7,8], Lies H. Hoefsloot[2], Cor W.R.J. Cremers[1], Frans P.M. Cremers[2,3], Uwe Wolfrum[6], Marlies Knipper[5], Ronald Roepman[2,3,†] and Hannie Kremer[1,*,†]

[1]Department of Otorhinolaryngology, [2]Department of Human Genetics, Radboud University Nijmegen Medical Centre, [3]Nijmegen Centre for Molecular Life Sciences, Nijmegen, The Netherlands, [4]Department of Pharmacology and Anatomy, Rudolf Magnus Institute of Neuroscience, University Medical Centre Utrecht, Utrecht, The Netherlands, [5]Department of Otorhinolaryngology, Hearing Research Centre Tübingen, THRC, Molecular Neurobiology, University of Tübingen, Tübingen, Germany, [6]Department of Cell and Matrix Biology, Institute of Zoology, Johannes Gutenberg University of Mainz, Mainz, Germany and [7]Unidad de Genética y Diagnóstico Prenatal, Hospital Universitario La Fe and [8]Departamento de Genética, Universidad de Valencia, Valencia, Spain

Received November 17, 2005; Revised and Accepted January 18, 2005

Mutations in the *DFNB31* gene encoding the PDZ scaffold protein whirlin are causative for hearing loss in man and mouse. Whirlin is known to be essential for the elongation process of the stereocilia of sensory hair cells in the inner ear, though its complete spatial and temporal expression patterns remained elusive. Here, we demonstrate that, in embryonic development, the gene is not only expressed in the inner ear, but also in the developing brain and the retina. Various isoforms of whirlin are widely and differentially expressed, and we provide evidence that whirlin directly associates with USH2A isoform b and VLGR1b, two proteins that we previously reported to be part of the Usher protein interactome. These proteins co-localize with whirlin at the synaptic regions of both photoreceptor cells and outer hair cells in the cochlea. These findings indicate that whirlin is part of a macromolecular PDZ protein scaffold that functions in the organization of the pre- and/or postsynaptic side of photoreceptor and hair cell synapses. Whirlin might be involved in synaptic adhesion through interaction with USH2A and VLGR1b as well as in synaptic development as suggested by its spatial and temporal expression patterns. In addition, we demonstrate that whirlin, USH2A and Vlgr1b co-localize at the connecting cilium and the outer limiting membrane of photoreceptor cells and in spiral ganglion neurons of the inner ear. Our data show that whirlin is connected to the dynamic Usher protein interactome and indicate that whirlin has a pleiotropic function in both the retina and the inner ear.

INTRODUCTION

Mutations in the *DFNB31/WHRN* gene encoding whirlin are causative for DFNB31, a non-syndromic profound type of recessive hearing loss (1,2). The whirler (*wi*) mouse with a recessive mutation in *Whrn* exhibits auditory and vestibular dysfunction and stereocilia elongation is impaired (3). At embryonic day 18.5 (E18.5), the stereocilia of cochlear inner hair cells (IHCs) are already significantly shorter than in control mice. Elongation has a normal rate until postnatal day 1, but prematurely stops between postnatal days 1 and 4 (3).

*To whom correspondence should be addressed at: Department of Otorhinolaryngology, Radboud University Nijmegen Medical Centre, Internal Postal Code 377, PO Box 9101, 6500 HB Nijmegen, The Netherlands. Tel: +31 243610487; Fax: +31 243668752; Email: h.kremer@antrg.umcn.nl
†The authors contributed equally to this work.

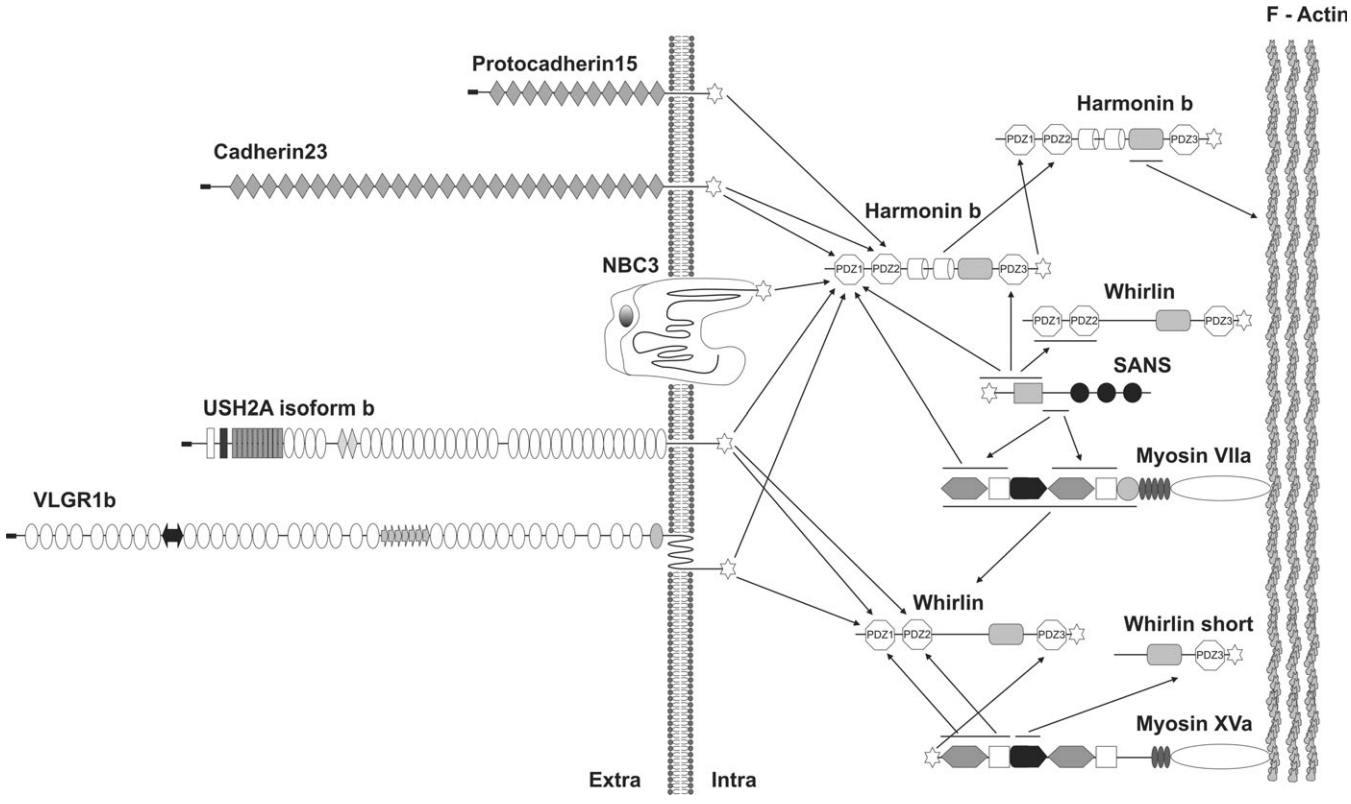

Figure 1. Schematic representation of so far identified associations between components of the Usher protein interactome (13,14,16–18). Myosin XVa is included as an interaction partner of whirlin. Arrows and lines mark the interacting regions of the proteins. The association between whirlin and SANS was determined in a yeast two-hybrid assay (van Wijk and Kalay, unpublished data).

Whirlin was shown to be transiently present at the tip of stereocilia during the elongation process in both IHC and outer hair cells (OHCs) in the cochlea, at the tips of stereocilia of vestibular hair cells (1,4,5) and also at the base of stereocilia (4). Different isoforms of whirlin are differentially expressed in IHCs and OHCs (1). The motor protein myosin XVa interacts with whirlin, which is essential for the localization of whirlin at the tip of the stereocilia (Fig. 1) (4,6). The whirlin–myosin XVa connection explains that in the shaker-2 mouse with a mutated *Myo15a* gene the stereocilia defect is very similar to that in the whirler mouse with shorter stereocilia and a diminished staircase pattern (7). In man, mutations in the *MYO15A* gene cause severe to profound hearing loss (DFNB3) (8). The whirlin–myosin XVa complex might indirectly regulate the actin polymerization at the stereocilia tips and thereby contribute to the programmed stereocilia elongation.

A second type of developmental stereocilia aberration is a defective cohesion of the stereocilia. This is caused by mutations in the genes encoding cadherin 23, protocadherin 15, harmonin, myosin VIIa and the very large G-protein coupled receptor 1 (Vlgr1) resulting in hearing loss and vestibular dysfunction (9–11; references therein). Mutations in the human orthologs of these genes are involved in Usher syndrome (USH) characterized by hearing impairment and retinitis pigmentosa. In type I (USH1) and III (USH3) also vestibular function is impaired (reviewed in 12). The scaffold protein harmonin, encoded by the gene involved in USH type IC (USH1C), interacts with all known USH1 proteins and the USH2 proteins, USH2A isoform b and VLGR1b, and is regarded to be the key organizer of the Usher protein interactome that functions at specific sites in photoreceptor cells and hair cells (13–18). Harmonin is a scaffold protein with three PDZ (postsynaptic density 95, PSD-95; discs large, Dlg; zonula occludens-1, ZO-1) (19) domains in isoforms a and b, two in the N-terminal and one in the C-terminal part of the protein. This three-PDZ-domain structure of harmonin is highly homologous to that of whirlin. Recently, we have shown that also USH2A isoform b, VLGR1b and the USH2B candidate protein NBC3 are part of this Usher protein interactome in both inner ear and retina (18). On the basis of the structural homology with harmonin and expression in the inner ear and central nervous system, we regarded whirlin as a candidate for interaction with the USH2 proteins and NBC3. We here report that whirlin can directly interact with the USH2 proteins VLGR1b and USH2A isoform b, but not with NBC3. Furthermore, RNA *in situ* hybridization (ISH) provided evidence that whirlin is differentially expressed in the brain, the retina and the cochlea throughout development. Immunohistochemistry showed that whirlin co-localizes with the USH2 proteins at the synaptic terminals and the connecting cilium of photoreceptor cells and at the synaptic terminals of OHC in the cochlea. Our data support the hypothesis that the Usher proteins are part of a dynamic Usher protein interactome that fulfills several functions at

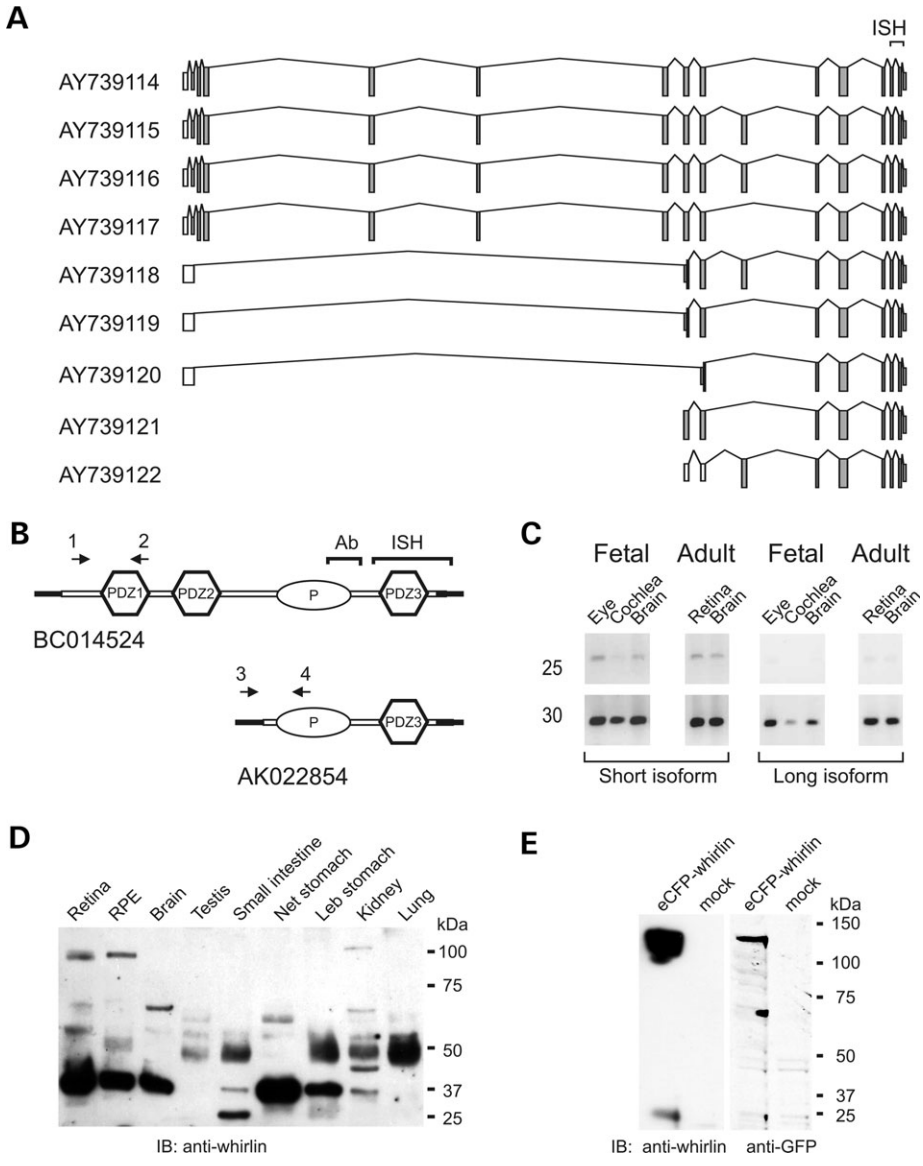

Figure 2. Structure and expression profile of whirlin. (**A**) Whrn isoforms that were identified by Belyantseva *et al*. (6). The long isoforms encode PDZ1, 2 and 3, whereas the short isoforms encode PDZ3. (**B**) Protein structure of whirlin, showing the long (BC014524) and short (AK022854) isoforms. The positions of the primers (nos 1–4), the region that was used as antigen in antibody production (Ab) and the region that corresponds to the antisense riboprobe for RNA ISH are indicated. (**C**) Expression profile using semi-quantitative RT–PCR of *DFNB31* in fetal, as well as adult eye (retina), ear (cochlea) and brain. The expression levels were compared using specific primers to amplify a fragment of either the long or the short isoform of *DFNB31*, using either 25 or 30 PCR cycles. Both isoforms of *DFNB31* were expressed in all analyzed tissues. (**D**) Detection of whirlin on a multiple tissue immunoblot of bovine protein extracts, using a specific polyclonal antibody against whirlin. (**E**) Detection of recombinant eCFP–whirlin on an immunoblot of COS-1 cell lysates by the antibody against whirlin (lane 1), as well as an antibody against GFP, recognizing the eCFP epitope tag (lane 3). The antibodies did not detect a signal in the lysates from mock-transfected cells (lanes 2 and 4), indicating their specificity.

different sites in the neurosensory cells of the retina and the cochlea and suggest that *DFNB31* is a candidate gene for USH as it is 'guilty by association'.

RESULTS

Whirlin is broadly, but differentially, expressed

The distribution of expressed sequence tags of whirlin in the UniGene database in the human (UniGene Hs.93836) and mouse (UniGene Mm.300397) gene clusters indicates that the gene is broadly, but not ubiquitously expressed. As the UniGene data do not reveal the tissue distribution of the different whirlin splice variants that were previously identified in mouse (6) (Fig. 2A) and human (1) (Fig. 2B), we raised a specific antibody against amino acids 701–765 of whirlin, a region present in all known isoforms (Fig. 2B), and analyzed the protein expression of whirlin on a multiple tissue blot of bovine protein extracts (Fig. 2D). Although western blot analysis showed expression of whirlin in all tissues analyzed, the number, size and intensity of the signals corresponding to specific protein bands varied considerably between the

tissues. The strongest signal in many tissues, corresponding to a protein size of 40 kDa, was found in all tissues tested, except for lung and testis. The size of this band does not correspond to any of the known splice variants. However, only for mouse cochlea, an extensive characterization of splice variants was performed. Alternatively, this 40 kDa isoform might be species-specific or the predominance of isoforms exhibits species-specificity. A 65 kDa band could be identified in retina, brain and kidney, whereas signals corresponding to the full-length protein (98 kDa) were detected only in retina, retinal pigment epithelium (RPE) and kidney (Fig. 2D). In addition, a 49 kDa band that was previously described (5) was detected in RPE, testis, small intestine, stomach, kidney and lung, and a specific smaller variant of 25 kDa was identified only in small intestine. Subsequently, we analyzed, by semi-quantitative RT–PCR, whether the *DFNB31* variants encoding the 'long' isoforms (Fig. 2A, isoforms 1–4) or the 'short' isoforms (Fig. 2A, isoforms 5–9) show differences in expression levels in human eye, ear and brain at embryonic or adult stages. For this purpose, gene-specific primers were used that amplified fragments of either the long variants (Fig. 2B, primers 1 and 2) or the short variants of *DFNB31* (Fig. 2B, primers 3 and 4). We found that both isoforms were expressed at very similar levels, both in fetal and adult tissues, and showed little tissue variability (Fig. 2C).

Whirlin expression is prominent at distinct neural layers during development

As whirlin was found to be expressed in different tissues both at embryonic and adult stages, we used RNA ISH to more accurately determine the spatial and temporal expression patterns of the gene in mice (Fig. 3). The murine antisense probe that was used recognized all known variants of Whrn (Fig. 2A). The sense probe did not show any specific signals, indicating the specificity of the experiments (data not shown). Whirlin expression was first detected at embryonic day 10.5 (E10.5), in the basal plate of the spinal cord, in the ventral neural epithelium of the developing brain and in the region of the lung bud (Fig. 3A). At E12.5, *Whrn* is expressed in the complete neuroepithelium except for the neocortex. Regions of the developing central nervous system with a strong signal are the ventral epithelium of the fourth ventricle, the ventral epithelium of the midbrain, the developing striatum and the optic recess (Fig. 3B). In the developing eye, *Whrn* expression is detected in the inner neuroblastic layer (Fig. 3D). At E14.5, *Whrn* expression was detected in the intervertebral cartilage, the cortex of the developing kidney, the tongue, the region of the urethra and strongly in specific regions of the brain, e.g. striatum, optic recess, ventral tegmental area, roof of the midbrain, choroid plexus of the lateral ventricles and the fourth ventricle (Fig. 3C). The developing neocortex is devoid of expression. At this timepoint, expression is first notable in the inner ear in the developing maculae of the saccule and the utricle, in the cristae of the semicircular canals and in the vestibulocochlear ganglion (Fig. 3J). In the developing neural retina, a strong signal was present in the inner neuroblastic layer (Fig. 3E). At E16.5, expression of whirlin was very similar to that at E14.5 and could furthermore be clearly distinguished in the neuroepithelium (Fig. 3F). Also, in the neocortex, expression was visible at this stage in the intermediate zone (data not shown). In addition to expression in the cortex of the kidney, expression was detected in the thymus (data not shown). The last embryonic timepoint of our analysis was E18.5, where the expression was mainly as in E16.5 (Fig. 3K and L). In the cochlea, a weak signal was now detected in the developing sensory epithelium (data not shown). Expression in the ganglion layers of the retina decreased and was no longer detected in the innermost region of these layers (Fig. 3G). From postnatal day 7 (P7) onwards (Fig. 3H and I), also the developing photoreceptor cells express whirlin.

Whirlin is integrated in the Usher protein network by direct interaction with USH2A and VLGR1, but not with NBC3

The consistent expression of the *DFNB31* gene in the neural retina and cochlea throughout development, and the structural homology between whirlin and harmonin suggested a link to the Usher protein network. We previously identified that the PDZ domains of the USH1C protein harmonin interact with the class I PDZ-binding motifs (PBMs) of other USH1 proteins (13,16,17) and with the class I PBMs at the C-terminus of the cytoplasmic domains of NBC3 and the USH2 proteins USH2A and VLGR1b (18). The scaffolding protein harmonin and its protein 'cargo' is thus recruited to the cytoplasmic face of the cell membrane. Bioinformatic analysis of the PDZ domains of harmonin using RANKPROP (20) and sequence alignments identified that whirlin is the nearest homolog of harmonin, with their PDZ1, 2 and 3 domains being 40, 47 and 23% identical, respectively (Fig. 4A). We therefore performed protein–protein interaction studies to analyze the putative association of the three PDZ domains of whirlin with the intracellular 'tail' fragments of USH2A (139 amino acids), VLGR1b (150 amino acids) and NBC3 (96 amino acids), containing the C-terminal class I PBMs (Fig. 4C–F).

We tested whether there was a direct interaction by carrying out *in vitro* glutathione *S*-transferase (GST) pull-down assays (Fig. 4C). We identified that 6 × His-tagged full-length whirlin was pulled down efficiently from COS-1 cell lysates by the GST-fused cytoplasmic tail domains of USH2A and VLGR1b, but not by the GST-NBC3_tail or only GST.

Using yeast two-hybrid assays, we identified that full-length whirlin, as well as only its PDZ1 domain, interacts with the C-terminal part of USH2A and VLGR1b, but not with NBC3 (Fig. 4D). Deletion of the last six amino acids that contained the conserved C-terminal class I PBM (Fig. 4B) fully disrupted the interaction with PDZ1. The PDZ2 domain of whirlin also showed some binding capacity towards USH2A that was disrupted by deleting the PBM, but interaction with VLGR1b or NBC3 could not be detected. The C-terminal PDZ3 domain of whirlin was not able to bind to any of the three proteins.

To complement these results in a mammalian cell-based assay, epitope-tagged full-length whirlin and the cytoplasmic tail domains of USH2A, VLGR1b and NBC3 were expressed in COS-1 cells. We performed immunoprecipitation assays using anti-flag antibodies and were able to show that

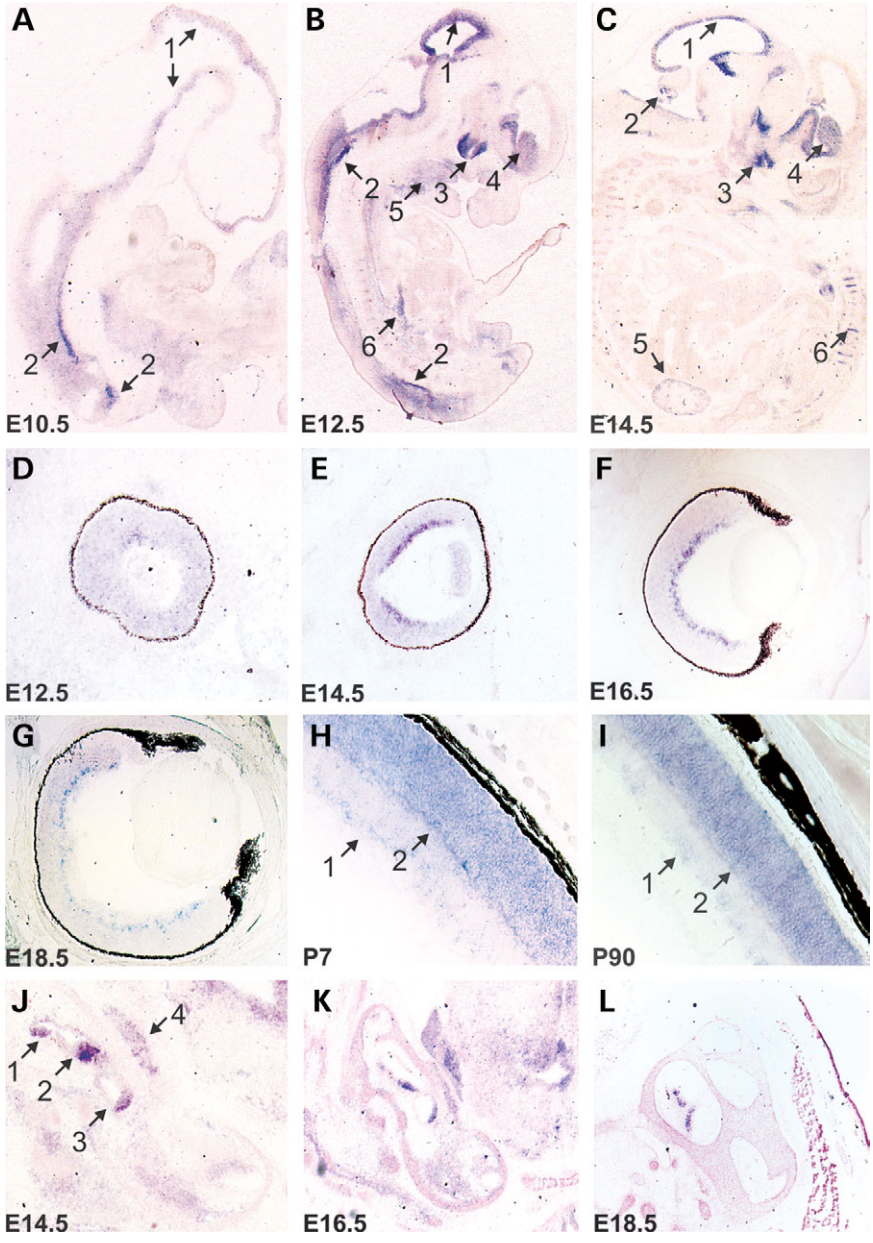

Figure 3. *Whrn* RNA in embryonic and adult mouse. Localization of *Whrn* expression by RNA ISH on cryosections of mouse embryos of different developmental stages with a probe that recognizes all reported *Whrn* splice variants (Fig. 2A). In sagittal whole embryo cryosections, specific expression was found in the following structures (indicated by numbers and arrows). (**A**) E10.5: 1, neural epithelium with strongest staining in the ventral neural epithelium; 2, basal plate of the spinal cord. (**B**) E12.5: staining of the neuro-epithelium except the neocortex; 1, roof of the midbrain; 2, basal plate of the spinal cord; 3, region of the optic recess; 4, striatum; 5, tongue: 6, lung. (**C**) E14.5: 1, roof of the midbrain; 2, choroid plexus of the fourth ventricle; 3, optic recess; 4, corpus striatum; 5, cortex of the kidney; 6, intervertebral cartilage. (**D**–**G**) Embryonic development of the eye at E12.5 (D), in which *Whrn* expression begins in the inner neuroblastic layer of the retina. At E14.5 (E) and E16.5 (F), *Whrn* is expressed in the inner neuroblastic layer of the retina, and at E18.5 (G), *Whrn* expression is limited to a subset of the ganglion cells. (**H** and **I**) Maintained expression of *Whrn* at postnatal day 7 (P7) (H) and p90 eye. Expression was seen in a subset of the ganglion cells (1) and is also detectable in the photoreceptor cells (2) at P7 (H) and P90 (I). (**J**–**L**) Coronal sections of the developing inner ear at E14.5 (J) with *Whrn* expression in the crista, a semicircular canal (1), the maculae of the utricle (2) and the saccule (3) and the vestibulocochlear ganglion (4). At E16.5 (K) and E18.5 (L), *Whrn* expression was maintained in the vestibular system. At E18.5, very weak expression was detected in the developing neurosensory epithelium of cochlea (data not shown).

full-length hemagglutinin (HA)-whirlin co-immunoprecipitated with flag-USH2A_tail (Fig. 4E, lane 1) and flag-VLGR1b_tail (Fig. 4E, lane 2), but not with flag-NBC3_tail (Fig. 4E, lane 3) and the unrelated protein flag-STRAD (Fig. 4E, lane 4). Reciprocal immunoprecipitation experiments using anti-HA antibodies confirmed these results (Fig. 4F).

We were able to visualize the interaction in these cells using fluorescence microscopy with different monomeric fluorescent protein epitope tags. We fused the different proteins at their N-terminus to either monomeric red fluorescent protein (mRFP) or enhanced cyan fluorescent protein (eCFP), variants that are fully separated in their emission spectra. We showed

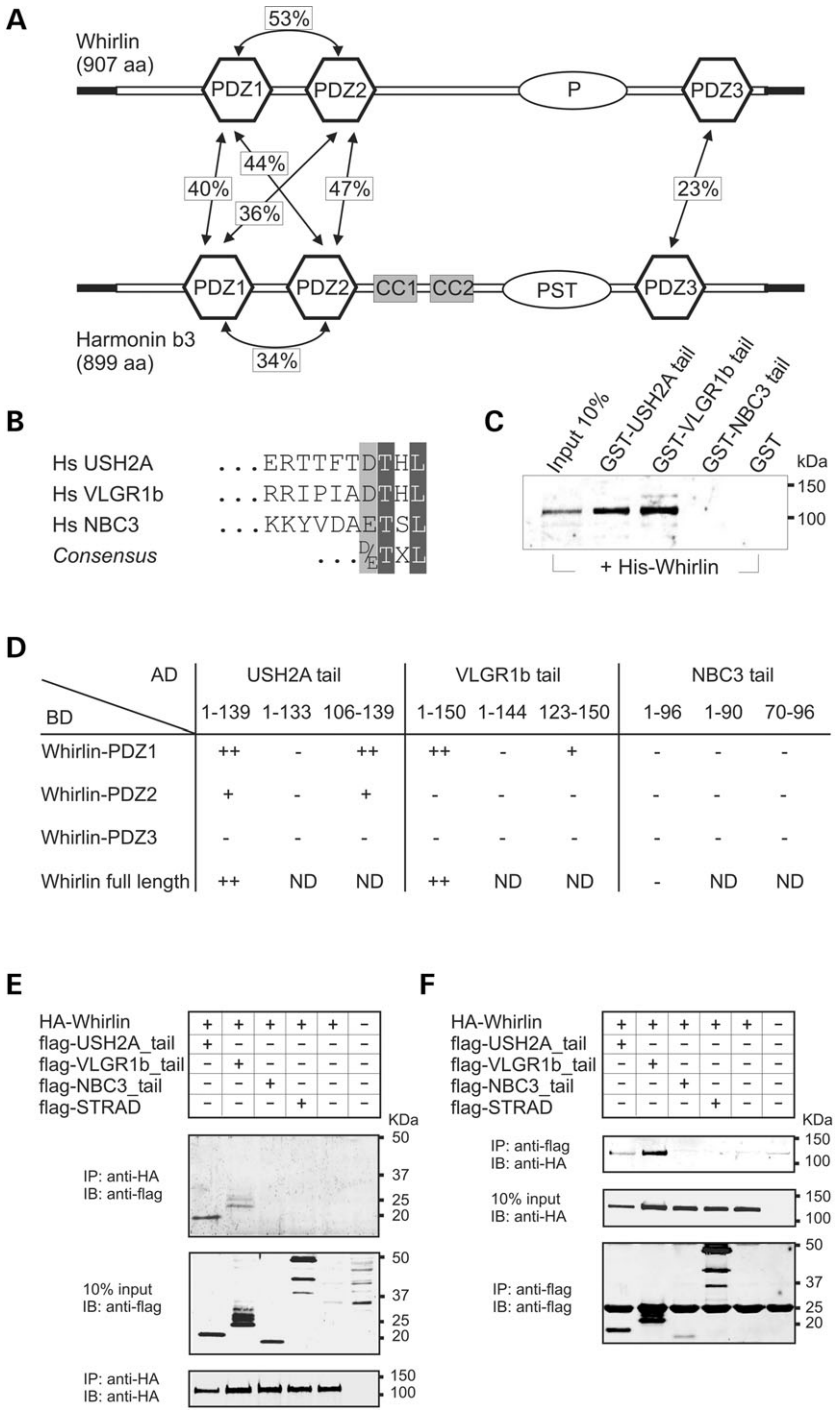

Figure 4. Whirlin physically interacts through PDZ–PBM association with USH2A and VLGR1b. (**A**) Identities between the three PDZ domains of harmonin and whirlin. (**B**) Sequence alignment of the class I PBM in the cytoplasmic tails of USH2A, VLGR1b and NBC3. (**C**) GST pull-down analysis, showing that $(His)_6$-tagged whirlin was efficiently pulled down by GST-USH2A_tail (lane 2) and by GST-VLGR1b_tail (lane 3), but not by GST–NBC3_tail (lane 4) or unfused GST (lane 5), as detected by an anti-$(His)_6$ antibody. The first lane shows 10% of the input protein lysate. (**D**) Yeast two-hybrid analysis of the interaction between the three PDZ domains of whirlin and the cytoplasmic tails of USH2A, VLGR1b and NBC3. The HIS3, MEL1 and LacZ reporter genes were either strongly activated (++), weakly activated (+), not activated (−) or not determined (ND). The PDZ1 and PDZ2 domains interacted with USH2A, the PDZ1 domain interacted with VLGR1b and whirlin was not found to interact with NBC3. (**E** and **F**) Co-immunoprecipitation of whirlin with USH2A and VLGR1b, but not with NBC3. (E) The immunoblot (IB) in the top panel shows that flag-USH2A_tail (lane 1) and flag-VLGR1b_tail (lane 2) co-immunoprecipitated with HA-whirlin, whereas flag-NBC3_tail (lane 3) and the unrelated protein flag-STRAD (lane 4) or mock-transfected cell lysate (lane 5) did not. Protein input is shown in the middle panel; the anti-HA immunoprecipitates are shown in the bottom panel. (F) Reciprocal immunoprecipitation assay. The immunoblot (IB) in the top panel revealed that HA-whirlin (input shown in the middle panel) co-immunoprecipitated with flag-USH2A_tail (lane 1) and with flag-VLGR1b_tail (lane 2), but not with flag-NBC3_tail (lane 3) and the unrelated protein flag-STRAD (lane 4) or mock-transfected cell lysate (lane 5). The anti-flag immunoprecipitates are shown in the bottom panel.

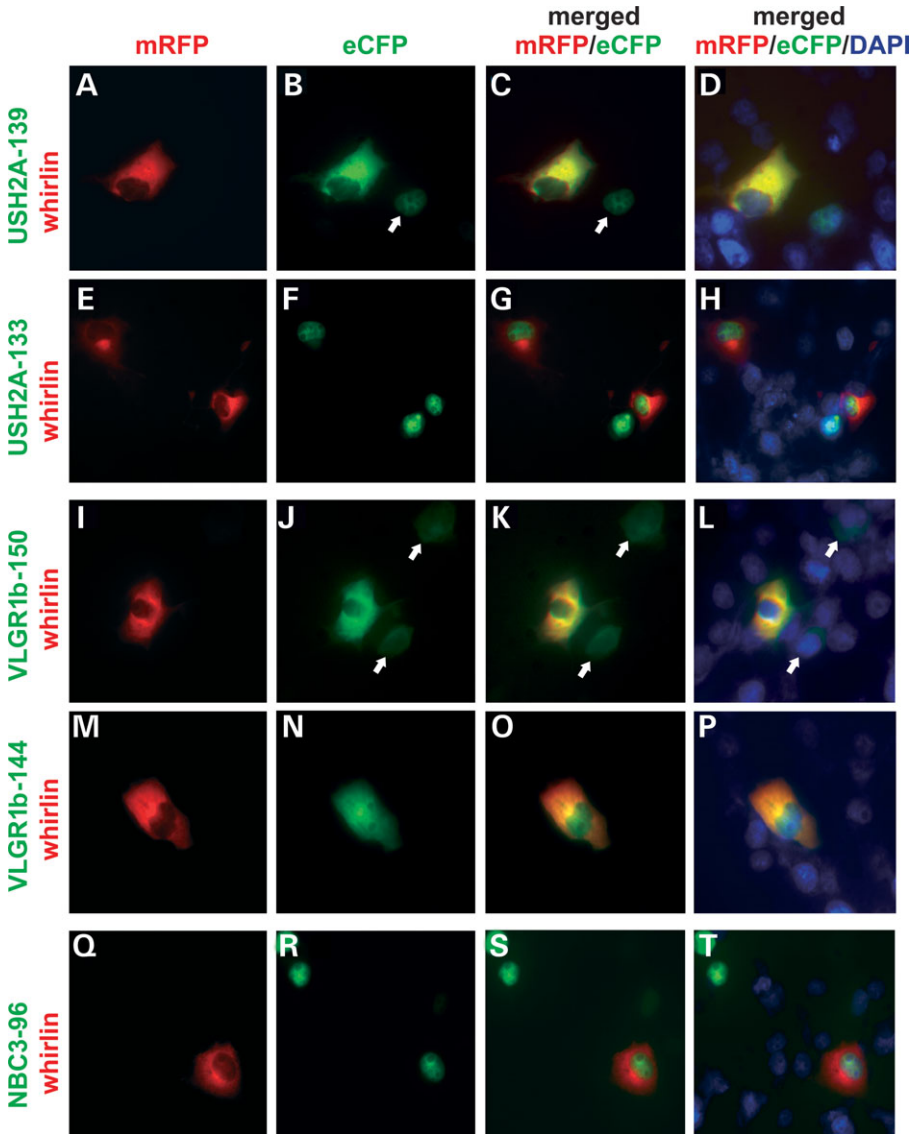

Figure 5. Whirlin co-localized with the cytoplasmic tails of USH2A and VLGR1b, but not with NBC3 upon overexpression in COS-1 cells. (**A**, **E**, **I**, **M**, **Q**) mRFP–whirlin (red signal) was localized in the cytoplasm, which was not affected by co-expression of USH2A (**B**–**D**) The eCFP–USH2A tail region (139 amino acids, green signal) was localized in the cell nucleus when singly transfected [arrows in (B) and (C)], but when co-expressed with whirlin, both proteins were localized in the cytoplasm [yellow signal in overlays (C) and (D)]. (**F**–**H**) The USH2A tail region without the PBM (133 amino acids, green signal) was localized in the cell nucleus, also when co-expressed with whirlin. (**J**–**L**) The eCFP–VLGR1b tail region (150 amino acids, green signal) was localized both in the cell nucleus as well as in the cytoplasm when singly transfected [faint signal, arrows in (J–L)], but when co-expressed with whirlin, both proteins were localized in the cytoplasm only [yellow signal in overlays (K) and (L)]. (**N**–**P**) The VLGR1b tail region without the PBM (144 amino acids, green signal) was localized in the cell nucleus and in the cytoplasm, also when co-expressed with whirlin. (**R**–**T**) The NBC3 tail region (96 amino acids, green signal) was localized in the cell nucleus, also when co-expressed with whirlin.

that in COS-1 cells expressing the full-length whirlin fused to mRFP, the protein was localized in the cytoplasm (Fig. 5A, red signal). In cells only transfected with the cytoplasmic tail domain of USH2A fused to eCFP, the protein was specifically localized in the nucleus (Fig. 5B and C, green signal), suggesting that a cryptic nuclear localization signal in this peptide may underlie translocation to the nucleus. Co-expression of whirlin with USH2A fully retained the latter to the cytoplasm, as no nuclear signal could be detected in these cells (Fig. 5C and D, yellow signal), and resulted *in vivo* in the co-localization of both proteins. Removal of the last six amino acids, containing the PBM, fully disrupted the retention of USH2A by whirlin in the cytoplasm, as in cells co-expressing both proteins, all of the USH2A_tail proteins were found in the nucleus, whereas whirlin was present in the cytoplasm (Fig. 5E–H). In these cells, no yellow signal could be identified in the overlays (Fig. 5G and H). In COS-1 cells, co-expressing whirlin and VLGR1b_tail, the situation was similar (Fig. 5I–P). VLGR1b localized both in the cytoplasm and in the nucleus (Fig. 5J and K), and in cells where it was co-expressed with whirlin, the protein was maintained in the cytoplasm only (Fig. 5K and L, yellow signal in

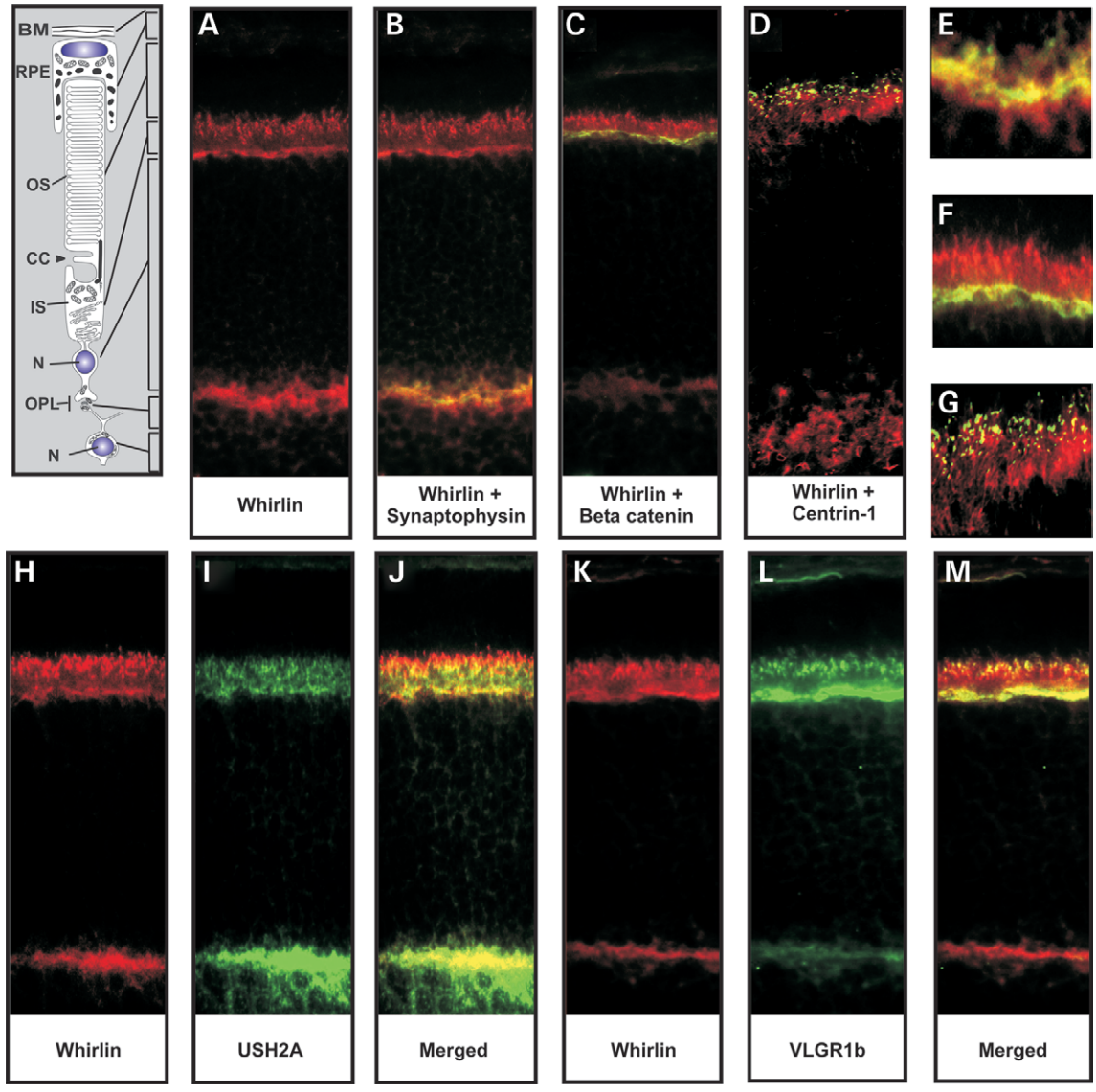

Figure 6. Whirlin co-localizes with USH2A and VLGR1b in the retina. (**A**–**G**) Subcellular localization of whirlin in radial cryosections of adult (P20) rat retinae using anti-whirlin antibodies (red signal) and antibodies against specific markers of retinal cell layers (green signal). (A) Immunostaining of whirlin indicates localization at the connecting cilium (CC), the inner segments (IS), the outer limiting membrane and the outer plexiform layer (OPL). (B) Co-immunostaining of whirlin and synaptophysin, a marker of the synapses of the outer plexiform layer, showing co-localization at this specific layer (yellow signal). (C) Co-localization (yellow signal) of whirlin and β-catenin, a marker of the outer limiting membrane, the adherence junctions with the Müller glia cells at the base of the inner segments. (D) Co-localization (yellow signal) in mouse retina of whirlin and centrin-1, a marker of the connecting cilia. (E–G). Details of the subcellular localization of whirlin in, respectively, (B–D). (**H**–**J**) are, respectively, rat retinal sections immunostained with anti-whirlin, anti-USH2A and an overlay of (H) and (I). (J) Co-localization (yellow signal) of USH2A and whirlin at the outer plexiform layer, the outer limiting membrane, the inner segments and partly at the connecting cilium. (**K**–**M**) are, respectively, rat retinal sections immunostained with anti-whirlin, anti-VLGR1b and an overlay of (K) and (L). (M) Co-localization (yellow signal) of USH2A and VLGR1b at the outer limiting membrane, the connecting cilium and more weakly at the outer plexiform layer and the inner segments.

overlay). Deletion of the PBM of VLGR1b again allowed translocation of the protein to the nucleus (Fig. 5N–P). However, co-expressing whirlin with the cytoplasmic tail domain of NBC3, also containing a class I PBM, did not affect the nuclear localization of the latter (Fig. 5Q–T), as no yellow signal could be observed in the overlays (Fig. 5S and T).

USH2A and VLGR1 co-localize with whirlin in the retina

As the RNA ISH experiments revealed the expression of *DFNB31* in the photoreceptor cells, we set out to identify the subcellular localization of the whirlin protein and its newly identified interactors USH2A and VLGR1 in the retina. The above described specific polyclonal antibody against whirlin, recognizing both long and short isoforms in the retina (Fig. 2B), was used to stain unfixed cryosections of adult rat retinas. Whirlin exhibited specific expression in the outer plexiform layer, in the photoreceptor inner segments and, very prominently, in the outer limiting membrane and connecting cilia (Fig. 6A). Markers for these specific structures revealed specific co-localization with the neuroendocrine marker synaptophysin in the pre-synaptic layer of the outer

plexiform layer (Fig. 6B and E), with the outer limiting membrane marker β-catenin (Fig. 6C and F) and with the connecting cilium marker centrin (Fig. 6D and G). The staining towards whirlin was highly specific because it was fully blocked by pre-incubation of the primary antibodies with the cognate peptide epitope, and pre-immune serum gave no signal (data not shown). Co-immunostaining of retinal sections with antibodies against whirlin and USH2A revealed co-localization of both interacting proteins, with the highest expression of both proteins at the outer plexiform layer and outer limiting membrane, and only a limited co-localization in the connecting cilium, at the basal side (Fig. 6H–J). Co-immunostaining experiments of retinal sections with antibodies against whirlin and VLGR1b also indicated that these proteins co-localize, with the highest expression of both proteins at the outer limiting membrane and connecting cilium (Fig. 6K–M).

USH2A and VLGR1 co-localize with whirlin in the inner ear

Immunohistochemistry with antibodies directed against the intracellular regions of USH2A and VLGR1b was performed to address co-localization and thus interaction of these proteins with whirlin in the cochlea. At rat postnatal day 26 (P26), whirlin is located at the synaptic terminals of OHCs (Fig. 7A–C) where it co-localizes with both USH2A and VLGR1b (Fig. 7D–G). In IHCs, a co-localization in synaptic regions was only detected for USH2A and VLGR1b as was previously described (18) (Fig. 7H and I). No whirlin positive signals were seen at VLGR1b positive synaptic sites at the IHC level (Fig. 7I, compare H and I, open arrow). Whirlin was detected in stereocilia of both IHCs (Fig. 7H) and OHCs (Fig. 7G), despite earlier reports describing the disappearance of the protein from the stereocilia at the end of elongation (5). This might be due to an isoform of whirlin that is not recognized by the antibodies used by Kikkawa *et al*. (5). Alternatively, mouse and rat might differ in spatio-temporal expression of whirlin isoforms. No USH2A and VLGR1b immunostaining could be detected in the stereocilia of both OHCs and IHCs at this age, when stereocilia are fully developed. Speckled immunostaining of whirlin was seen in the stria vascularis (data not shown). Analogous to immunostaining of neuronal cell bodies and nerve fibers in the brain (21), immunofluorescence with anti-whirlin antibodies was detected in the nerve fibers at the habenula perforata (Fig. 7N), in the auditory nerve (Fig. 7O) and in the spiral ganglia neuronal cell bodies where whirlin co-localizes with USH2A and VLGR1b (Fig. 7J–L).

DISCUSSION

In this study, we demonstrate that during embryogenesis, the *Whrn* gene is predominantly expressed in the developing brain, the eye and the inner ear. We furthermore show that whirlin directly interacts with the cytoplasmic tails of USH2A isoform b and VLGR1b and that these proteins co-localize at distinct sites in OHCs of the cochlea and in photoreceptor cells. As we have previously shown that the latter two proteins associate with members of the USH1 protein complex (15,18), our findings likely reflect and expand the molecular diversity of the Usher protein interactome and its role in ear and eye function.

The earliest embryonic expression of *Whrn* was detected at E10.5, most prominently in the ventral aspects of the neural epithelium. Interestingly, this matches the RNA *in situ* expression pattern of *Vlgr1* (22). The localization in the ventricular zones suggests a role in neuronal proliferation. It is tempting to speculate that VLGR1b and whirlin already function in the same protein complex very early in neural development. In the early embryonic stages, similar to *Vlgr1*, *Whrn* expression is very low in the region that develops into the neocortex, whereas a high expression in the optic stalk could be observed. Both *Whrn* and *Vlgr1* are also highly expressed in the developing eye, albeit the *Whrn* transcription at the early developmental stages of the retina is limited to the inner neuroblastic layer, whereas *Vlgr1* transcripts are detected pan-retinal (22). The developmental expression pattern of *Ngl-1*, identified as an interacting protein of whirlin (4) also partially overlaps with that of *Whrn*. Transcripts of both genes are found in the striatum, but expression in the retina and in the cerebral cortex diverges, as *Ngl-1* is abundantly detected in the outer neuroblastic layer and in the cerebral cortex (23), where *Whrn* is absent. Transcription of *Whrn* in the eye is first observed at E12.5 in the innermost layers of the neural retina. At this stage, nerve fibers originate from the primitive ganglion cells and grow towards the inner surface of the optic cup. In the developing photoreceptor cells, *Whrn* expression was first detected at postnatal stages of development (P7), when also a subpopulation of the ganglion cells exhibit staining in RNA ISH. In the inner ear, the earliest transcription was found at E14.5 in the maculae of utricle and saccule that have differentiated from the surrounding tissue at this stage and in developing cristae of the semicircular canals. Both the supporting cells and the precursors of the sensory cells were stained. Transcription was also detected in the vestibulocochlear ganglion from E14.5 onwards. Thus, whirlin functions in the developing neurosensory elements of the eye and the inner ear and, in addition, in ganglion cells of the inner ear.

In the adult neurosensory tissues of the eye and the inner ear, specific antibodies against whirlin enabled us to detect whirlin expression at distinct subcellular sites. Interestingly, expression was detected in the synaptic regions of the sensory cells, both in the retina and in the cochlea. Hair cells and photoreceptor cells possess ribbon synapses, sites where synaptic vesicles are organized along an electron dense ribbon (24). These structures are specific for neurons that transmit graded signals such as photoreceptor cells, bipolar neurons, hair cells and pinealocytes (25). However, as whirlin was detected in the OHC synaptic regions that contain ribbon synapses only in the more apical turns of the cochlea (26) and not in the IHC synaptic regions that in all turns contain the ribbon synapse, it seems unlikely that whirlin is a component of this specialized synaptic vesicle organizer but merely has a more general role in the organization of the synapse or in synaptic vesicle transmission. This is corroborated by the fact that whirlin, also described as CIP-98, was shown to interact with CASK in adult rat brain via its PDZ3 region (21). CASK is described to function in exocytosis of synaptic vesicles (27,28), in the alignment of

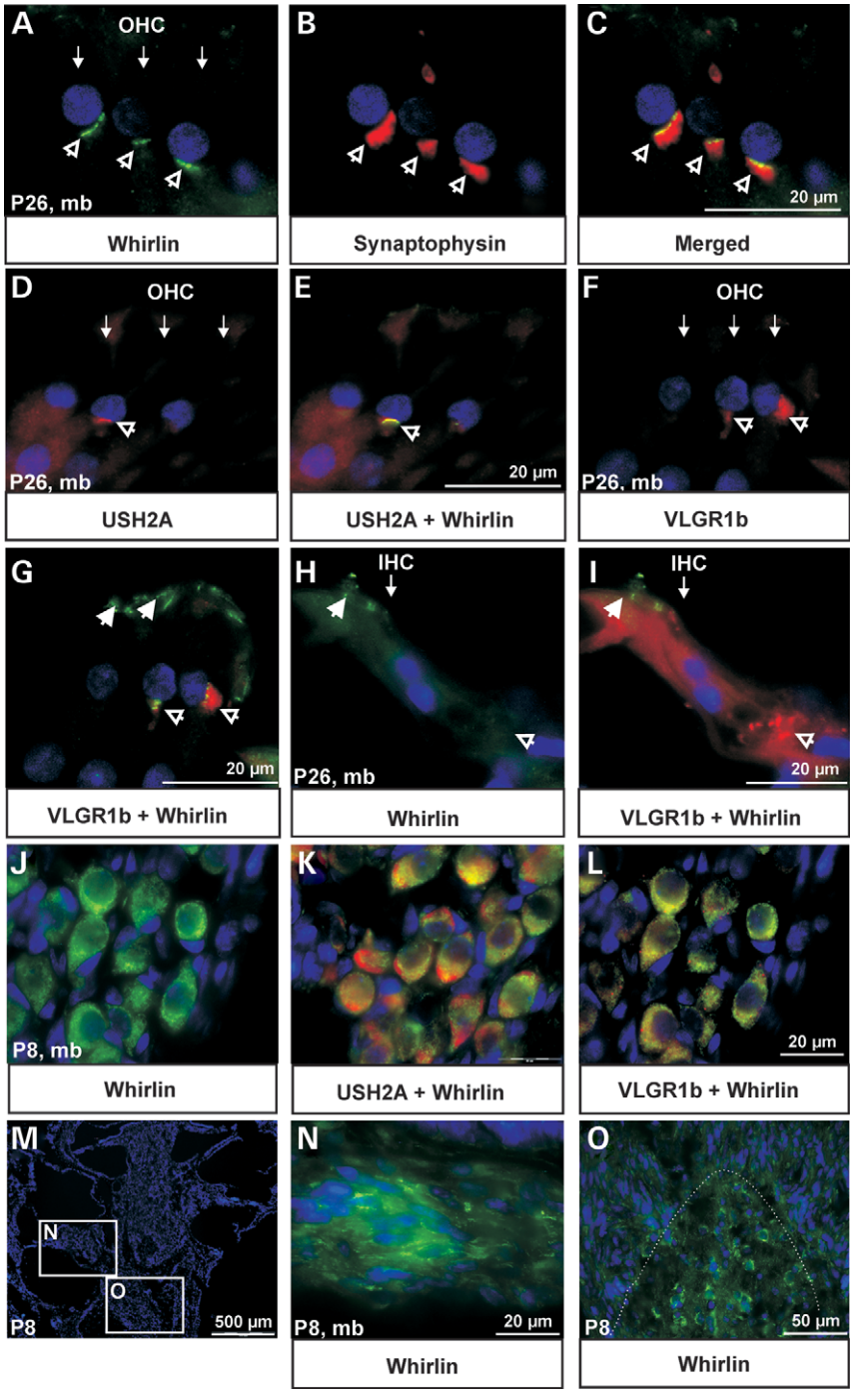

Figure 7. Whirlin co-localizes with USH2A and VLGR1b in the inner ear of P8/P26 adult rats. (**A**–**C**) Whirlin co-localizes with synaptophysin in the synaptic region of OHCs. There, whirlin also co-localizes with USH2A and VLGR1b (**D**–**G**). In IHCs, whirlin could only be detected in the stereocilia. It does not localize at the synaptic region of IHCs, where VLGR1b and USH2A (data not shown) are present (**H** and **I**). Whirlin is also located in the stereocilia of both IHC and OHC at this age (A–I). In the spiral ganglia, whirlin co-localizes with both USH2A and VLGR1b at the cell bodies (**J**–**L**). (**M**–**O**) The nerve fibers show immunostaining with anti-whirlin antibodies at the habenula perforata (M and N) and the cochlear nerve (M–O). m, middle turn of the cochlea; mb, mid-basal region of the cochlea. Open arrowheads point towards the synaptic region of hair cells, filled arrowheads towards the stereocilia.

the pre- and postsynaptic machinery through interaction with neurexin and in targeting *N*-methyl-D-aspartate receptors (reviewed in 29). Because the OHCs are mainly innervated by efferent terminals, the whirlin staining pattern in the inner ear might suggest a participation of whirlin in the synaptic organization or transmission in the efferent terminals. The co-localization of the PDZ proteins harmonin and whirlin, and the USH2A, VLGR1b and NBC3 proteins, differentially interacting through PDZ–PBM binding at the synaptic terminals in the retina and cochlea (present data) (18) suggests

that these PDZ protein scaffolds organize heterogeneous ensembles of proteins, similar to other synaptic PDZ scaffolds (e.g. PSD-95) (reviewed in 29). The developmental expression pattern of *Whrn*, the protein–protein interaction data and subcellular protein localizations we present here suggest that the composition of these PDZ scaffolds could change at different locations in the cell, both during development and in response to, for example, neuronal activity. At the synaptic regions, they could be essential for controlling the structure, strength and plasticity of the synapses. The scaffolding of USH2A isoform b and VLGR1b with large extracellular regions might contribute to structure and strength of the synapse through homophilic or heterophilic interactions in the organization of the synaptic cleft, as has been suggested for cadherin 23 and protocadherin 15 (13,15,17,30). Whirlin might also contribute to the organization of ion channels in the pre- and/or postsynaptic membrane as was shown for other scaffolding proteins (reviewed in 29).

Besides at the outer plexiform layer, whirlin, USH2A and VLGR1b co-localize at the connecting cilium of photoreceptor cells, as confirmed by the co-localization of whirlin with the connecting cilium marker centrin 1 at this subcellular site (31). The connecting cilium, together with the outer segment, originates from a non-motile primary cilium and remains in mature photoreceptors as the connecting link between the inner segments and outer segments (32). The outer segments contain the light-sensory stacked membrane disks that are turned over at a high rate, but do not possess organelles for protein and lipid synthesis. These are all located in the inner segments, and all inner segments–outer segments translocations are dependent on the connecting cilium, using mechanisms comparable to intra flagellar transport. Besides protein transport, the connecting cilium is essential for disk morphogenesis, possibly through its role in the dynamics of the F-actin network at the distal part of the connecting cilium (33). Dysfunction of components of the connecting cilium and cilia, in general, are causative for both syndromic and non-syndromic forms of retinal degeneration such as Leber congenital amaurosis type 6 (LCA6) (34), retinitis pigmentosa type 1 (RP1) (35), retinitis pigmentosa type 3 (RP3) (36), USH1B (37) Senior–Løken syndrome (38) and Bardet–Biedl syndrome (39) (reviewed in 40). In analogy to the PDZ scaffolds of the synapses, the USH2A–VLGR1b–whirlin protein scaffold might play a role in anchoring the connecting cilium to the surrounding interphotoreceptor matrix and thus maintaining its structure and plasticity or/and providing additional anchoring points for translocation of other proteins that bind to the intracellular regions of USH2A isoform b and VLGR1b to the connecting cilium (van Wijk, unpublished data). Interestingly, the Usher protein myosin VIIa (USH1B), SANS (USH1G) and cadherin 23 (USH1D) are localized to the connecting cilium (41). Myosin VIIa, which interacts with whirlin (4), is known to function in protein transport along the connecting cilium (32,42). The scaffold protein SANS (USH1G) and cadherin 23 (USH1D) might be another link between USH proteins and basal bodies and thus the connecting cilium. Our data suggest that dysfunction of the connecting cilium in addition to dysfunction of photoreceptor synapses could be a major factor underlying the RP phenotype in USH.

In the inner ear, whirlin was already shown to be essential for elongation of the stereocilia for which interaction with myosin XVa is a prerequisite (1,4–6). Mutations in the *DFNB31* gene cause pre-lingual hearing loss (DFNB31), whereas *Whrn*$^{-/-}$ mutant mice are profoundly deaf and exhibit defects in stereocilia formation, identified already at E18. No visual impairment has been reported to be associated with mutations in the whirlin gene in man and mouse, which seems unexpected given the expression of whirlin from early retina development until adulthood as revealed in our study. As the age of the patients in the two DFNB31 families has not been reported, it cannot be excluded that they will still develop retina dysfunction later in life or that there might be subclinical retinal dysfunction. The absence of visual impairment in the whirler mouse has analogy to that in the mice mutated for the USH1 genes (41). Striking, however, fact is that the two known *DFNB31* mutations, as well as the *wi* mutation of the whirler mouse, are located downstream of the region encoding PDZ1 and PDZ2, and thus are not disrupting the domains interacting with USH2A and VLGR1b. Using an antibody against whirlin on a multiple tissue, immunoblot did detect multiple specific signals, corresponding to isoforms of different size. We therefore suggest that a short isoform of whirlin, containing PDZ1 and PDZ2, might be sufficient for retina function analogous to the rescue of the defect of stereocilia growth by the short C-terminal isoform of whirlin (1) and that only mutations that affect the expression of a functional PDZ1 or PDZ2 will lead to a retinal phenotype. Although mutation analysis of the *DFNB31* gene by sequencing exons and exon–intron boundaries in 20 USH1 patients did not reveal disease causing mutations in the gene (data not shown), we propose that in addition to causing deafness, mutations in *DFNB31* could cause USH as well as isolated retinal degenerations, though likely in a limited number of cases. It would therefore be worthwhile to screen a larger patient panel with other types of USH and patients with non-syndromic retinal degeneration for mutations in the *DFNB31* gene.

The lack of a retinal phenotype in both man and mice with a defect in the *DFNB31/Whrn* gene could also be explained by functional redundancy, as we previously showed co-localization of USH2A and VLGR1b with harmonin in the synaptic region of photoreceptor cells (18). It would furthermore be interesting to elucidate whether harmonin and whirlin interact via PDZ–PBM interaction and thereby show functional redundancy at these sites. This apparently does not play a role in the inner ear because mutations in either whirlin or harmonin lead to congenital hearing loss.

The identification reported here that whirlin is a novel PDZ scaffold protein in the Usher protein interactome, expressed both in the ear and the eye throughout development, suggests that whirlin mediates multiple biological processes that are vital for development and function of these sensory organs.

MATERIALS AND METHODS

Animals

In this study, Wistar rats, guinea pigs and C57B6 JOlaHsd mice (Harlan, The Netherlands), housed in standard cages

and receiving water and food *ad libitum*, were used. Animal experiments were conducted in accordance with the international and institutional guidelines.

Antibodies and plasmids

The anti-whirlin antibodies were raised in guinea pigs against a GST-fusion protein encoding a fragment (amino acids 701–765) of the long isoform of the whirlin protein. The antibodies against the cytoplasmic tails of USH2A and VLGR1b, centrin1 (clone 20H5) and synaptophysin were previously described (18). The anti-NBC3 antibody was derived from Alpha Diagnostic (USA). Anti-HA and anti-flag antibodies were derived from Sigma (Germany). Secondary antibodies for immunohistochemistry and western blot analysis were derived from Molecular Probes-Invitrogen (Carlsbad, CA, USA), Rockland (Philadelphia, PA, USA) and Jackson ImmunoResearch Laboratories (USA). cDNAs encoding the human cytoplasmic tails or part of it, with or without PDZ type I binding motif of USH2A, VLGR1b and NBC3 were cloned in the pDONR201 vector as described before (18). cDNA fragments of *DFNB31* transcripts were amplified with IMAGE clone IRAUp969F0450D (RZPD, Germany) as a template. By using Gateway technology (Invitrogen), cDNAs encoding human full-length whirlin (amino acids 1–907), PDZ1 (amino acids 138–233), PDZ2 (amino acids 279–360) and PDZ3 (amino acids 819–907) were cloned in the pDONR201 vector as previously described (18).

Yeast two-hybrid analysis

A GAL4-based yeast two-hybrid system (HybriZAP, Stratagene, USA) was used to identify the interactions between whirlin and USH2A, VLGR1b and NBC3 according to methods previously described (43) with minor variations. As a host, yeast strain PJ69-4A was used (44), which carried the *HIS3* (histidine), *ADE2* (adenine), *MEL1* (α-galactosidase) and *LacZ* (β-galactosidase) reporter genes. Interactions were analyzed by assessment of reporter gene activation, through growth on selective media (*HIS3* and *ADE2* reporter genes), an X-α-gal colorimetric plate assay (*MEL1* reporter gene) and an X-β-gal colorimetric filter lift assay (*LacZ* reporter gene).

GST pull-down

In order to produce GST-fusion proteins, BL21-DE3 cells were transformed with pDEST15-USH2A_tail (amino acids 5064–5202), pDEST15-VLGR1b_tail (amino acids 6157–6307) or pDEST15-NBC3_tail (amino acids 1119–1214). Cells were induced at 30°C for 4 h with 0.5 mM IPTG and subsequently lysed with STE buffer [1% Sarkosyl, 1% Triton X-100, 5 mM 1,4-dithiothreitol (DTT)] supplemented with protease inhibitor cocktail (Roche, Germany). Lysates were incubated at 4°C for 16 h with glutathione–Sepharose 4B beads (Amersham Biosciences, USA). Beads with fusion proteins bound to it were extensively washed with lysis buffer and TBSTD (TBS with 1% Triton X-100 and 2 mM DTT) at 4°C. The amount of GST-fusion protein attached to the Sepharose beads was verified on a 10% SDS–PAGE gel stained with Gelcode Blue Stain Reagent (Pierce, USA). His-tagged whirlin was produced by transfecting COS-1 cells with pcDNA4-HisMax-Whirlin using Nucleofector kit V (Amaxa, USA), program A-24 according to manufacturer's instruction. The pre-cleared supernatant was incubated overnight at 4°C with equal amounts of blocked beads with GST or beads with GST-fusion proteins. After several washes with lysis buffer, the beads were boiled in 1 × SDS sample buffer, and proteins were resolved in SDS–PAGE and detected by western blot analysis.

Co-immunoprecipitation in COS-1 cells

HA-tagged whirlin was expressed by using the mammalian expression vector pcDNA3-HA/DEST and the flag-tagged intracellular tails of all three USH2A, NBC3 and VLGR1b by using p3xflag-CMV/DEST from the Gateway cloning system (Invitrogen). Both plasmids contain a CMV promoter. COS-1 cells were transfected by using the Nucleofector kit V (Amaxa, USA) and program A-24, according to manufacturer's instructions. Twenty-four hours after transfection, cells were washed with phosphate-buffered saline (PBS) and subsequently lysed on ice in lysis buffer [50 mM Tris–HCl pH 7.5, 150 mM NaCl, 1% Triton X-100 supplemented with complete protease inhibitor cocktail (Roche)]. HA-tagged whirlin was immunoprecipitated from cleared lysates overnight at 4°C by using anti-HA polyclonal antibody and Protein A/G PLUS–Sepharose (Santa Cruz Biotechnology, USA), whereas flag-tagged USH2A_tail, VLGR1b_tail and NBC3_tail were immunoprecipitated by using monoclonal anti-flag M2 Agarose beads (Sigma). After four washes in lysis buffer, the protein complexes were analyzed on immunoblots using the Odyssey Infrared Imaging System (LI-COR, USA). Tagged molecules were detected by anti-HA or anti-flag mono- or polyclonal antibodies. As secondary antibodies, IRDye800 goat-anti-mouse IgG and Alexa Fluor 680 goat-anti-rabbit IgG were used.

Co-localization in COS-1 cells

To determine the cellular localization of the cytoplasmic tails of human USH2A, VLGR1b and NBC3 as well as full-length whirlin (Genbank NM_015404) in COS-1 cells, we cloned cDNAs encoding the tails of USH2A, VLGR1b and NBC3 in pDEST501 by using the Gateway cloning technology (Invitrogen), resulting in N-terminally fused eCFP–USH2 and eCFP–NBC3 fusion proteins. Whirlin was cloned in pDEST733, resulting in an N-terminally fused mRFP–whirlin fusion protein. COS-1 cells were co-transfected with pDEST501-USH2A tail, pDEST501-VLGR1b tail or pDEST501-NBC3 tail, together with pDEST733-whirlin by using Lipofectamine (Invitrogen) according to manufacturer's instructions. Twenty-four hours after transfection, cells were washed with PBS, fixed with 4% paraformaldehyde and mounted with Vectashield containing DAPI (Vector Laboratories, Inc., UK). Images were taken with an Axioplan2 Imaging fluorescence microscope (Zeiss) equipped with a DC350FX camera (Zeiss) and processed using Adobe Photoshop (Adobe Systems, USA).

Western blot analysis from bovine tissue protein extracts

Parts of bovine tissues were isolated and frozen in liquid nitrogen. Tissues were homogenized by using the mikrodismembrator (Braun Biotech International, USA) for 2 min at 1000 r.p.m. Homogenized tissues were lysed with lysis buffer [50 mM Tris–HCl pH 7.5, 150 mM NaCl, 0.5% Triton X-100 supplemented with complete protease inhibitor cocktail (Roche)] and subsequently centrifuged for 10 min at 11000*g* at 4°C. Supernatants were analyzed by SDS–PAGE and western blotting.

Immunohistochemistry in tissue

Unfixed eyes of 20-day-old (P20) Wistar rats were isolated and frozen in melting isopentane. For cochlear immunohistochemistry, cochleae from P8 and P26 rats were isolated, dissected and fixed as described before (45). After fixation, cochleae were decalcified in Rapid Bone Decalcifier (Fisher-Scientific, Germany). Cryosections were made at a thickness of 10 μm and treated with 0.01% Tween-20 in PBS followed by a blocking step with blocking solution (0.1% ovalbumin, 0.5% fish gelatin in PBS). Antibodies diluted in blocking solution were incubated overnight at 4°C. Secondary antibodies were also diluted in blocking solution and incubated together with DAPI for 1 h. Sections were embedded with Prolong Gold Anti-fade (Molecular Probes). Pictures were made with an Axioskop2 Mot plus fluorescence microscope (Zeiss) equipped with an AxioCam MRC5 camera (Zeiss). Images were processed using Axiovision 4.3 (Zeiss) and Adobe Photoshop (Adobe Systems). Pre-immune serum did not give specific staining and antibodies blocked with the antigen also resulted in complete lack of signal.

Expression profiling

The expression of the known isoforms of whirlin was examined by performing RT–PCR analysis on RNA from human fetal and adult tissues as described before (46). Primers used for the detection of the transcripts encoding the long isoform(s) consisting of PDZ1, PDZ2 and PDZ3 (Genbank NM_015404) are 5′-TGCTCTTCGACCAATACACG-3′ and 5′-CAGACAGCACCAGCTTCTTG-3′. For detection of the isoform(s) consisting of the proline-rich region and PDZ3 (GenBank AK022854), the following primers were used: 5′-CACGATGCATGGTTCTCTTG-3′ and 5′-TGTTGAG CAGCTTGAACAGG-3′.

Digoxigenin labeling of cRNA ISH probes

For generating a probe, which recognizes transcripts for both the long and short isoform(s) of whirlin, part of the common 3′ end of the transcripts of whirlin was amplified using 5′-GGTCCGTGTGAGGAAAAGTG-3′ as a forward primer and 5′-GATAGGCTGGGAGTGCAAAG-3′ as a reversed primer. Murine retina cDNA was used as a template. The obtained PCR product was subsequently cloned in the pCR4-TOPO vector (Invitrogen) by using the TOPO cloning kit (Invitrogen). A PCR was performed by using T7 and T3-polymerase specific primers. Digoxigenin (DIG)-cRNA probes were generated by incubating 400 ng of PCR product with 2 μl 10× DIG RNA labeling mix (Roche), 2 μl T3 (sense) or T7 (antisense)-dependent RNA polymerase (Roche), 2 μl 10× Transcription buffer (Roche) and RNase-free H_2O added to a final volume of 20 μl, at 37°C for 2 h. To stop the reaction, 2 μl 0.2 M EDTA (pH 8.0) was added. The cRNA probe was ethanol precipitated and dissolved in RNase-free H_2O. Probe DIG concentrations were determined by dot blot analysis on Hybond N+ nylon membranes (Amersham Biosciences), compared with control DIG-cRNA probe (Roche), and stored at −80°C.

RNA ISH

Mouse embryos were collected at various embryonic stages (E12.5–E18.5), frozen on crushed dry ice and stored at −80°C. The embryos were embedded in Tissue-Tek O.C.T. compound (Sakura Finetek, USA) and sagitally cut into 16 μm sections at temperatures of −16 to −20°C. Sections were collected on SuperFrost Plus microscope slides (Menzel-Gläser, Germany). After quickly drying the sections, they were stored at −80°C until further use. The DIG-labeled cRNA probes were then hybridized to the mouse tissue sections as follows. Samples were rapidly defrosted and fixed in 4% paraformaldehyde in PBS (pH 7.4) for 10 min. Slides were washed three times in PBS (pH 7.4) and acetylated for 10 min in a solution containing 3.3 ml triethanolamine, 0.438 ml 37% fuming HCl, 0.625 ml acetic anhydride, in a final volume of 250 ml H_2O. Slides were washed three times for 5 min in PBS and pre-hybridized for 2 h at room temperature (RT) with hybridization mix [50% deionized formamide, 5 × SSC, 5 × Denhardt's solution, 250 μg/ml brewer's yeast tRNA (Roche) and 500 μg/ml sonicated salmon sperm DNA (Sigma)]. Subsequently, hybridization was performed overnight at 72°C with 150 μl hybridization mix containing 400 ng/ml DIG-labeled probe, washed briefly at 72°C in 2 × SSC and then washed for 2 h at 72°C in 0.2 × SSC. Slides were allowed to cool, transferred to 0.2 × SSC at RT for 5 min and subsequently transferred to buffer 1 [100 mM Tris–HCl, pH 7.4, 150 mM NaCl]. Slides were incubated for 1 h at RT with 10% heat inactivated fetal calf serum (FCS) in buffer 1, followed by overnight incubation at 4°C with 0.7 ml 1% heat inactivated FCS in buffer 1 with 1 : 5000 diluted anti-DIG-AP, fab fragment from sheep (Roche) per slide. Slides were washed three times in buffer 1 and once in buffer 2 [100 mM Tris–HCl, pH 9.5, 100 mM NaCl, 50 mM $MgCl_2$] at RT. One milliliter of staining solution [200 μl of NBT-BCIP stock solution (Roche) and 1 ml Levamisole (Sigma, 2.4 mg/ml) and 8.8 ml buffer 2 per 10 ml] was placed on the slides and staining was allowed to take place for 6 h to overnight in a dark environment. Subsequently, the slides were washed once in $T_{10}E_5$ [10 mM Tris, pH 8.0, and 5 mM EDTA] to stop the reaction. Slides were dehydrated and sealed using Entellan rapid mounting media (ProSciTech, Australia). Images were recorded on a Zeiss Axioskop2 plus microscope with a Sony power HAD DXC-950P 3CCD color video camera.

ACKNOWLEDGEMENTS

This study was supported by the Heinsius Houbolt Foundation, the Nijmegen ORL Research Fund, Oogfonds Nederland, Gelderse Blinden Vereniging, Stichting Blindenhulp, Algemene Nederlandse Vereniging ter Voorkoming van Blindheid, Rotterdamse Vereniging Blindenbelangen, Stichting voor Ooglijders, Dr F.P. Fischer-stichting, the DFG, Forschung contra Blindheit–Initiative Usher Syndrom, ProRetina Deutschland and the FAUN-Stiftung, Nürnberg.

Conflicts of Interest statement. There are no conflicts of interest.

REFERENCES

1. Mburu, P., Mustapha, M., Varela, A., Weil, D., El Amraoui, A., Holme, R.H., Rump, A., Hardisty, R.E., Blanchard, S., Coimbra, R.S. *et al*. (2003) Defects in whirlin, a PDZ domain molecule involved in stereocilia elongation, cause deafness in the whirler mouse and families with DFNB31. *Nat. Genet.*, **34**, 421–428.
2. Tlili, A., Charfedine, I., Lahmar, I., Benzina, Z., Mohamed, B.A., Weil, D., Idriss, N., Drira, M., Masmoudi, S. and Ayadi, H. (2005) Identification of a novel frameshift mutation in the *DFNB31/WHRN* gene in a Tunisian consanguineous family with hereditary non-syndromic recessive hearing loss. *Hum. Mutat.*, **25**, 503.
3. Holme, R.H., Kiernan, B.W., Brown, S.D. and Steel, K.P. (2002) Elongation of hair cell stereocilia is defective in the mouse mutant whirler. *J. Comp. Neurol.*, **450**, 94–102.
4. Delprat, B., Michel, V., Goodyear, R., Yamasaki, Y., Michalski, N., El Amraoui, A., Perfettini, I., Legrain, P., Richardson, G., Hardelin, J.P. *et al*. (2005) Myosin XVa and whirlin, two deafness gene products required for hair bundle growth, are located at the stereocilia tips and interact directly. *Hum. Mol. Genet.*, **14**, 401–410.
5. Kikkawa, Y., Mburu, P., Morse, S., Kominami, R., Townsend, S. and Brown, S.D. (2005) Mutant analysis reveals whirlin as a dynamic organizer in the growing hair cell stereocilium. *Hum. Mol. Genet.*, **14**, 391–400.
6. Belyantseva, I.A., Boger, E.T., Naz, S., Frolenkov, G.I., Sellers, J.R., Ahmed, Z.M., Griffith, A.J. and Friedman, T.B. (2005) Myosin-XVa is required for tip localization of whirlin and differential elongation of hair-cell stereocilia. *Nat. Cell Biol.*, **7**, 148–156.
7. Probst, F.J., Fridell, R.A., Raphael, Y., Saunders, T.L., Wang, A., Liang, Y., Morell, R.J., Touchman, J.W., Lyons, R.H., Noben-Trauth, K. *et al*. (1998) Correction of deafness in shaker-2 mice by an unconventional myosin in a BAC transgene. *Science*, **280**, 1444–1447.
8. Wang, A., Liang, Y., Fridell, R.A., Probst, F.J., Wilcox, E.R., Touchman, J.W., Morton, C.C., Morell, R.J., Noben-Trauth, K., Camper, S.A. and Friedman, T.B. (1998) Association of unconventional myosin MYO15 mutations with human nonsyndromic deafness DFNB3. *Science*, **280**, 1447–1451.
9. Frolenkov, G.I., Belyantseva, I.A., Friedman, T.B. and Griffith, A.J. (2004) Genetic insights into the morphogenesis of inner ear hair cells. *Nat. Rev. Genet.*, **5**, 489–498.
10. El Amraoui, A. and Petit, C. (2005) Usher I syndrome: unravelling the mechanisms that underlie the cohesion of the growing hair bundle in inner ear sensory cells. *J. Cell Sci.*, **118**, 4593–4603.
11. Johnson, K.R., Zheng, Q.Y., Weston, M.D., Ptacek, L.J. and Noben-Trauth, K. (2005) The Mass1frings mutation underlies early onset hearing impairment in BUB/BnJ mice, a model for the auditory pathology of Usher syndrome IIC. *Genomics*, **85**, 582–590.
12. Ahmed, Z.M., Riazuddin, S., Riazuddin, S. and Wilcox, E.R. (2003) The molecular genetics of Usher syndrome. *Clin. Genet.*, **63**, 431–444.
13. Boeda, B., El Amraoui, A., Bahloul, A., Goodyear, R., Daviet, L., Blanchard, S., Perfettini, I., Fath, K.R., Shorte, S., Reiners, J. *et al*. (2002) Myosin VIIa, harmonin and cadherin 23, three Usher I gene products that cooperate to shape the sensory hair cell bundle. *EMBO J.*, **21**, 6689–6699.
14. Siemens, J., Kazmierczak, P., Reynolds, A., Sticker, M., Littlewood-Evans, A. and Muller, U. (2002) The Usher syndrome proteins cadherin 23 and harmonin form a complex by means of PDZ-domain interactions. *Proc. Natl Acad. Sci. USA*, **99**, 14946–14951.
15. Reiners, J., Reidel, B., El Amraoui, A., Boeda, B., Huber, I., Petit, C. and Wolfrum, U. (2003) Differential distribution of harmonin isoforms and their possible role in Usher-1 protein complexes in mammalian photoreceptor cells. *Invest. Ophthalmol. Vis. Sci.*, **44**, 5006–5015.
16. Adato, A., Michel, V., Kikkawa, Y., Reiners, J., Alagramam, K.N., Weil, D., Yonekawa, H., Wolfrum, U., El Amraoui, A. and Petit, C. (2005) Interactions in the network of Usher syndrome type 1 proteins. *Hum. Mol. Genet.*, **14**, 347–356.
17. Reiners, J., Marker, T., Jurgens, K., Reidel, B. and Wolfrum, U. (2005) Photoreceptor expression of the Usher syndrome type 1 protein protocadherin 15 (USH1F) and its interaction with the scaffold protein harmonin (USH1C). *Mol. Vis.*, **11**, 347–355.
18. Reiners, J., van Wijk, E., Marker, T., Zimmermann, U., Jurgens, K., te Brinke, H., Roepman, R., Knipper, M., Kremer, H. and Wolfrum, U. (2005) The scaffold protein harmonin (USH1C) provides molecular links between Usher syndrome type 1 and type 2. *Hum. Mol. Genet.*, **14**, 3933–3943.
19. van Ham, M. and Hendriks, W. (2003) PDZ domains-glue and guide. *Mol. Biol. Rep.*, **30**, 69–82.
20. Weston, J., Elisseef, A., Zhou, D., Leslie, C. and Noble, W.S. (2004) Protein ranking: from local to global structure in the protein similarity network. *Proc. Natl. Acad. Sci. USA*, **101**, 6559–6563.
21. Yap, C.C., Liang, F., Yamazaki, Y., Muto, Y., Kishida, H., Hayashida, T., Hashikawa, T. and Yano, R. (2003) CIP98, a novel PDZ domain protein, is expressed in the central nervous system and interacts with calmodulin-dependent serine kinase. *J. Neurochem.*, **85**, 123–134.
22. McMillan, D.R., Kayes-Wandover, K.M., Richardson, J.A. and White, P.C. (2002) Very large G protein-coupled receptor-1, the largest known cell surface protein, is highly expressed in the developing central nervous system. *J. Biol. Chem.*, **277**, 785–792.
23. Lin, J.C., Ho, W.H., Gurney, A. and Rosenthal, A. (2003) The netrin-G1 ligand NGL-1 promotes the outgrowth of thalamocortical axons. *Nat. Neurosci.*, **6**, 1270–1276.
24. Khimich, D., Nouvian, R., Pujol, R., Tom, D.S., Egner, A., Gundelfinger, E.D. and Moser, T. (2005) Hair cell synaptic ribbons are essential for synchronous auditory signalling. *Nature*, **434**, 889–894.
25. Sterling, P. and Matthews, G. (2005) Structure and function of ribbon synapses. *Trends Neurosci.*, **28**, 20–29.
26. Raphael, Y. and Altschuler, R.A. (2003) Structure and innervation of the cochlea. *Brain Res. Bull.*, **60**, 397–422.
27. Zhang, Y., Luan, Z., Liu, A. and Hu, G. (2001) The scaffolding protein CASK mediates the interaction between rabphilin3a and beta-neurexins. *FEBS Lett.*, **497**, 99–102.
28. Zordan, M.A., Massironi, M., Ducato, M.G., Te, K.G., Costa, R., Reggiani, C., Chagneau, C., Martin, J.R. and Megighian, A. (2005) Drosophila CAKI/CMG protein, a homolog of human CASK, is essential for regulation of neurotransmitter vesicle release. *J. Neurophysiol.*, **94**, 1074–1083.
29. Kim, E. and Sheng, M. (2004) PDZ domain proteins of synapses. *Nat. Rev. Neurosci.*, **5**, 771–781.
30. Bolz, H., Reiners, J., Wolfrum, U. and Gal, A. (2002) Role of cadherins in Ca^{2+}-mediated cell adhesion and inherited photoreceptor degeneration. *Adv. Exp. Med. Biol.*, **514**, 399–410.
31. Giessl, A., Pulvermuller, A., Trojan, P., Park, J.H., Choe, H.W., Ernst, O.P., Hofmann, K.P. and Wolfrum, U. (2004) Differential expression and interaction with the visual G-protein transducin of centrin isoforms in mammalian photoreceptor cells. *J. Biol. Chem.*, **279**, 51472–51481.
32. Besharse, J.C. and Horst, C.J. (2005) In Bloodgood, RA (ed.), *Ciliary and Flagellar Membranes*. New York, Plenum. pp. 389–417.
33. Chaitin, M.H., Schneider, B.G., Hall, M.O. and Papermaster, D.S. (1984) Actin in the photoreceptor connecting cilium: immunocytochemical localization to the site of outer segment disk formation. *J. Cell. Biol.*, **99**, 239–247.
34. Hong, D.H., Yue, G., Adamian, M. and Li, T. (2001) Retinitis pigmentosa GTPase regulator (RPGRr)-interacting protein is stably associated with the photoreceptor ciliary axoneme and anchors RPGR to the connecting cilium. *J. Biol. Chem.*, **276**, 12091–12099.
35. Ostrowski, L.E., Blackburn, K., Radde, K.M., Moyer, M.B., Schlatzer, D.M., Moseley, A. and Boucher, R.C. (2002) A proteomic

analysis of human cilia: identification of novel components. *Mol. Cell Proteomics*, **1**, 451–465.
36. Hong, D.H., Pawlyk, B.S., Shang, J., Sandberg, M.A., Berson, E.L. and Li, T. (2000) A retinitis pigmentosa GTPase regulator (RPGR)-deficient mouse model for X-linked retinitis pigmentosa (RP3). *Proc. Natl. Acad. Sci. USA*, **97**, 3649–3654.
37. Liu, X., Vansant, G., Udovichenko, I.P., Wolfrum, U. and Williams, D.S. (1997) Myosin VIIa, the product of the Usher 1B syndrome gene, is concentrated in the connecting cilia of photoreceptor cells. *Cell Motil. Cytoskeleton*, **37**, 240–252.
38. Otto, E.A., Loeys, B., Khanna, H., Hellemans, J., Sudbrak, R., Fan, S., Muerb, U., O'Toole, J.F., Helou, J., Attanasio, M. *et al.* (2005) Nephrocystin-5, a ciliary IQ domain protein, is mutated in Senior–Loken syndrome and interacts with RPGR and calmodulin. *Nat. Genet.*, **37**, 282–288.
39. Ansley, S.J., Badano, J.L., Blacque, O.E., Hill, J., Hoskins, B.E., Leitch, C.C., Kim, J.C., Ross, A.J., Eichers, E.R., Teslovich, T.M. *et al.* (2003) Basal body dysfunction is a likely cause of pleiotropic Bardet–Biedl syndrome. *Nature*, **425**, 628–633.
40. Eley, L., Yates, L.M. and Goodship, J.A. (2005) Cilia and disease. *Curr. Opin. Genet. Dev.*, **15**, 308–314.
41. Reiners, J., Nagel-Wolfrum, K., Jurgens, T., Marker, T. and Wolfrum, U. (2005) Molecular basis of the human Usher syndrome—deciphering the meshes of the Uhser protein network provides insights into the pathomechanisms of the Usher disease. *Exp. Eye Res.*, in press.
42. Liu, X., Udovichenko, I.P., Brown, S.D., Steel, K.P. and Williams, D.S. (1999) Myosin VIIa participates in opsin transport through the photoreceptor cilium. *J. Neurosci.*, **19**, 6267–6274.
43. Roepman, R., Schick, D. and Ferreira, P.A. (2000) Isolation of retinal proteins that interact with retinitis pigmentosa GTPase regulator by interaction trap screen in yeast. *Meth Enzymol.*, **316**, 688–704.
44. James, P., Halladay, J. and Craig, E.A. (1996) Genomic libraries and a host strain designed for highly efficient two-hybrid selection in yeast. *Genetics*, **144**, 1425–1436.
45. Knipper, M., Zinn, C., Maier, H., Praetorius, M., Rohbock, K., Kopschall, I. and Zimmermann, U. (2000) Thyroid hormone deficiency before the onset of hearing causes irreversible damage to peripheral and central auditory systems. *J. Neurophysiol.*, **83**, 3101–3112.
46. Luijendijk, M.W., van de Pol, T.J., van Duijnhoven, G., den Hollander, A.I., ten Caat, J., van Limpt, V., Brunner, H.G., Kremer, H. and Cremers, F.P. (2003) Cloning, characterization, and mRNA expression analysis of novel human fetal cochlear cDNAs. *Genomics*, **82**, 480–490.